

Synthesis and Characterization of a Novel Prostate Cancer-Targeted Phosphatidylinositol-3-kinase Inhibitor Prodrug

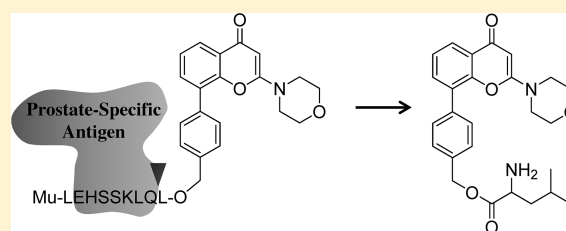
Daniele Baiz,[†] Tanya A. Pinder,[‡] Sazzad Hassan,[†] Yelena Karpova,[†] Freddie Salsbury,[#] Mark E. Welker,^{*,‡} and George Kulik^{*,†}

[†]Department of Cancer Biology and Comprehensive Cancer Center, Wake Forest School of Medicine, Medical Center Boulevard, Winston-Salem, North Carolina 27157, United States

[‡]Department of Chemistry, Wake Forest University, Winston-Salem, North Carolina 27109, United States

[#]Department of Physics, Wake Forest University, P.O. Box 7486, Winston-Salem, North Carolina 27109, United States

ABSTRACT: The phosphatidylinositol-3-kinase/Akt (PI3K/Akt) pathway is constitutively activated in a substantial proportion of prostate tumors and is considered a key mechanism supporting progression toward an androgen-independent status, for which no effective therapy is available. Therefore, PI3K inhibitors, alone or in combination with other cytotoxic drugs, could potentially be used to treat cancer with a constitutive activated PI3K/Akt pathway. To selectively target advanced prostate tumors with a constitutive activated PI3K/Akt pathway, a prostate cancer-specific PI3K inhibitor was generated by coupling the chemically modified form of the quercetin analogue LY294002 (HO-CH₂-LY294002, compound 8) with the peptide Mu-LEHSSKLQL, in which the internal sequence HSSKLQ is a substrate for the prostate-specific antigen (PSA) protease. The result is a water-soluble and latent PI3K inhibitor prodrug (compound 11), its activation being dependent on PSA cleavage. Once activated, the L-O-CH₂-LY294002 (compound 10) can specifically inhibit PI3K in PSA-secreting prostate cancer cells and induce apoptosis with a potency comparable to that of the original LY294002 compound.



INTRODUCTION

Prostate cancer remains the second leading cause of cancer-related death in men in the United States. Conventional treatments such as surgery, radiation, and androgen suppression are effective if prostate cancer is confined to the prostate. Unfortunately, many patients with advanced metastatic cancer treated with androgen ablation experience recurrence of androgen-independent cancer, with limited or transient response to other systemic chemotherapies.^{1,2} For this reason, there is an urgent need for new specific and targeted agents to treat androgen-independent prostate cancer. Several mechanisms have been proposed to explain why prostate cancer cells can grow in the absence or reduced presence of androgens. Recent papers suggest that the phosphatidylinositol 3-kinase/Akt (PI3K/Akt) pathway is one of the mechanisms that allow prostate cancer cells to maintain continued proliferation in a low-androgen environment.³

The PI3K pathway is a key signal transduction pathway initiated by receptor tyrosine kinases that recruit and activate the PI3K, resulting in an accumulation of phosphatidylinositol 3,4,5-triphosphate (PIP₃) in plasma membrane. This lipid second messenger recruits Akt and the phosphoinositide-dependent protein kinase 1 (PDK1) to the cell membrane, where Akt is phosphorylated by PDK1 at threonine 308. Activated Akt recruits the mammalian target of rapamycin (mTOR) that, acting with Rictor protein, forms the mTORC2 complex, which completes the activation of Akt by phosphorylation at serine 473. Fully activated Akt translocates to the

cytoplasm and nucleus, where it phosphorylates downstream substrates involved in angiogenesis, cell cycle progression, growth, migration, proliferation, and survival.⁴

Constitutive activation of the PI3K/Akt pathway in prostate cancer is often led by functional loss of the tumor suppressor PTEN (a phosphatase and tensin homologue deleted on chromosome 10) that dephosphorylates PI3K substrates or by activating mutations in the PI3 kinase itself that correlate with increased Akt phosphorylation, higher Gleason grade, advanced stage, and unfavorable prognosis.^{5,6} For these reasons, PI3K inhibitors have been considered as an adjuvant therapy for advanced prostate cancer; unfortunately, despite promising effects in preclinical models, recent clinical trials did not show benefits in prostate cancer-affected patients treated with PI3K inhibitors (source www.ClinicalTrials.gov).

One possible approach for improving the efficacy of PI3K inhibitors to treat prostate cancer patients may be to convert the PI3K inhibitor molecule into an inactive prodrug by attaching a specific prostate-specific antigen (PSA) cleavable peptide, increasing the delivery to tumor sites while minimizing systemic toxicity. PSA is a protease with chymotrypsin-like activity and is involved in the hydrolytic processing of semenogelins, which are necessary for seminal fluid liquefaction. In patients with prostate cancer, systemic PSA concentration is high, but inactive, in blood serum as PSA is

Received: June 22, 2012

Published: August 27, 2012

complexed with the α_1 -antichymotrypsin (PSA-ACT) or α_2 -macroglobulin.^{7,8} On the contrary, in the tumor environment, PSA is free (fPSA) and enzymatically active, able to activate cytotoxic prodrugs based on a PSA-cleavable peptidic sequence.⁹

In this work, we describe for the first time the synthesis and characterization of a prostate cancer-specific PI3K inhibitor prodrug based on the quercetin analogue LY294002 activated by PSA cleavage. On the basis of previous reports of anticancer toxins converted to PSA-activated prodrugs, we linked the PI3K inhibitor LY294002 with the Mu-LEHSSKLQL peptide, containing the HSSKLQ sequence specific for PSA cleavage.^{8,10–12} The generated PI3K inhibitor prodrug LY294002 (11) is water-soluble and is specifically activated in the media conditioned by the prostate cancer cells C4-2 that secrete PSA. Upon activation, the PI3K inhibitor prodrug 11 showed consistent time-dependent and concentration-dependent inhibition of the PI3 kinase and induction of apoptosis. The specificity of the PI3K inhibitor prodrug 11 for PSA-secreting prostate cancer cells was confirmed using the BT-549 breast cancer cell line and glioblastoma-astrocytoma U-87 MG cells, which do not produce PSA: in these cells the PI3K pathway activity is not affected by 11. Consistent with the requirement of cleavage by PSA for drug activation, PI3K/Akt signaling in BT-549 breast cancer cells is inhibited if 11 is previously incubated in C4-2 conditioned medium or in the presence of enzymatically active purified PSA.

Prostate tumor PSA-dependent inhibition of PI3K is expected to produce dual benefits for patients: by completely inhibiting the PI3K pathway at the tumor site and reducing side effects due to inhibition of PI3K in normal tissues, systemic exposure should be minimal, resulting only from the active drug being redistributed from the tumor.^{13,14}

DESIGN AND SYNTHESIS

PI3K Inhibitor Prodrug (Compound 11) Design. To generate a PI3K inhibitor prodrug activated by the prostate-specific antigen, we chose the quercetin analogue LY294002 (developed by Eli Lilly Co.). The stability of this agent in aqueous solutions made it a reagent of choice for numerous tissue culture studies of PI3K signaling. To determine the position in the LY294002 structure where an inhibitory peptide could be attached, we conducted modeling studies of interactions between the ATP binding pocket of the PI3 kinase and LY294002. These modeling studies have been performed using an existing crystal structure of the PI3 kinase to which LY294002 has been bound as a template.¹⁵ AutoDock3 software with AutoDock Tools was used to generate the appropriate charge, solvent, and van der Waals parameters for LY294002 and the PI3 kinase.¹⁶ Electrostatic and van der Waals potential grids for docking were generated on the basis of these parameters and were centered at the center of geometry for LY294002 in the crystal structure, although LY294002 was removed before grid creation.

To ensure both high resolution and sampling of a large region of protein for possible binding sites, the grids were generated at 0.375 Å resolution in a cube of 30 × 30 × 30 Å. LY294002 was redocked into the active site with 256 runs of AutoDock's Lamarckian genetic algorithm. Default parameters were used except in the number of runs (256) and the size of the initial pool (30000 initial dockings). Subsequent analysis showed that the LY294002 was docked with a similar pose as in the crystal structure with 4.0 μ M predicted affinity, using

AutoDock's estimator of binding affinity (Figure 1A, in blue).¹⁶ On the basis of this analysis, a phenyl ring in LY294002

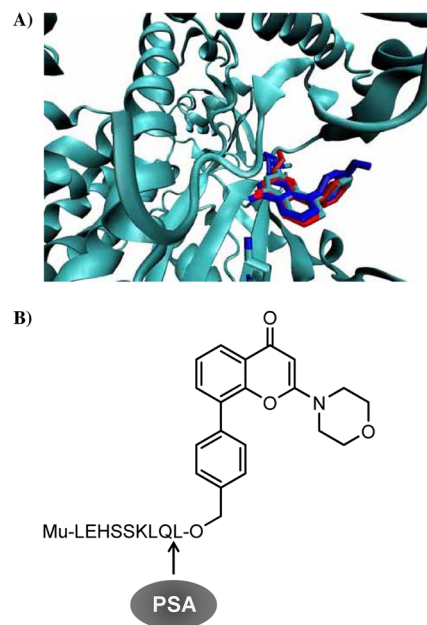


Figure 1. Modeling of the interaction between LY294002 derivative and PI3 kinase ATP-binding site. (A) Ribbon diagram of an X-ray structure of the PI3K ATP-binding site (gray) with LY294002. An active site Lys in bonds is shown for reference. Modeled structurally similar docking poses for LY294002 (blue) and 10 (red) are shown for comparison. (B) PI3K inhibitor prodrug (11) formula. Arrow points at predicted prostate-specific antigen cleavage site.

structure was identified to attach a CH_2OH moiety, which subsequently was used to couple the Mu-LEHSSKLQL sequence, containing the PSA substrate peptide (Figure 1B). Because PSA is predicted to cleave Mu-LEHSSKLQL peptide after glutamine (Q), it leaves leucine (L) attached to the phenyl ring of the LY294002 via the CH_2OH moiety. The AutoDock modeling of interaction between this “activated prodrug” 10 and PI3K has shown that it can still fit into the ATP binding site and, thus, is predicted to inhibit PI3K activity (Figure 1A, in red).

Synthesis of Compound 11. We synthesized 8-(4-(hydroxymethyl)phenyl)-2-morpholino-4H-chromen-4-one (8), an analogue of LY294002 containing a CH_2OH functional group, which should not adversely affect the PI3K binding ability but will permit the attachment of PSA substrate peptides (Figure 2A; numbers hereafter refer to structures in Figure 2). The synthesis of 8 was modeled after the synthetic strategy presented by Abbott and Thompson.¹⁷ Commercially available aromatic ester 2,3-dihydroxybenzoic acid (1) was converted to methyl 2,3-dihydroxybenzoate (2) by acid-catalyzed addition of methanol. The least sterically hindered hydroxyl was then converted to a triflate by treatment with trifluoromethylsulfonic anhydride to produce methyl-2-hydroxy-3-[[trifluoromethylsulfonyl]oxy]benzoate (3). The enolate of *N*-acetylmorpholine (4) was then generated with lithium diisopropyl amide and condensed with the ester in 3 to produce 2-hydroxy-3-(3-morpholin-4-yl-3-oxopropanoyl)phenyl trifluoromethanesulfonate (5). 5 underwent cyclodehydration after being treated with triflic anhydride to give 2-morpholin-4-yl-4-oxo-4H-chromen-8-yl trifluoromethanesulfonate (6). 6 was then

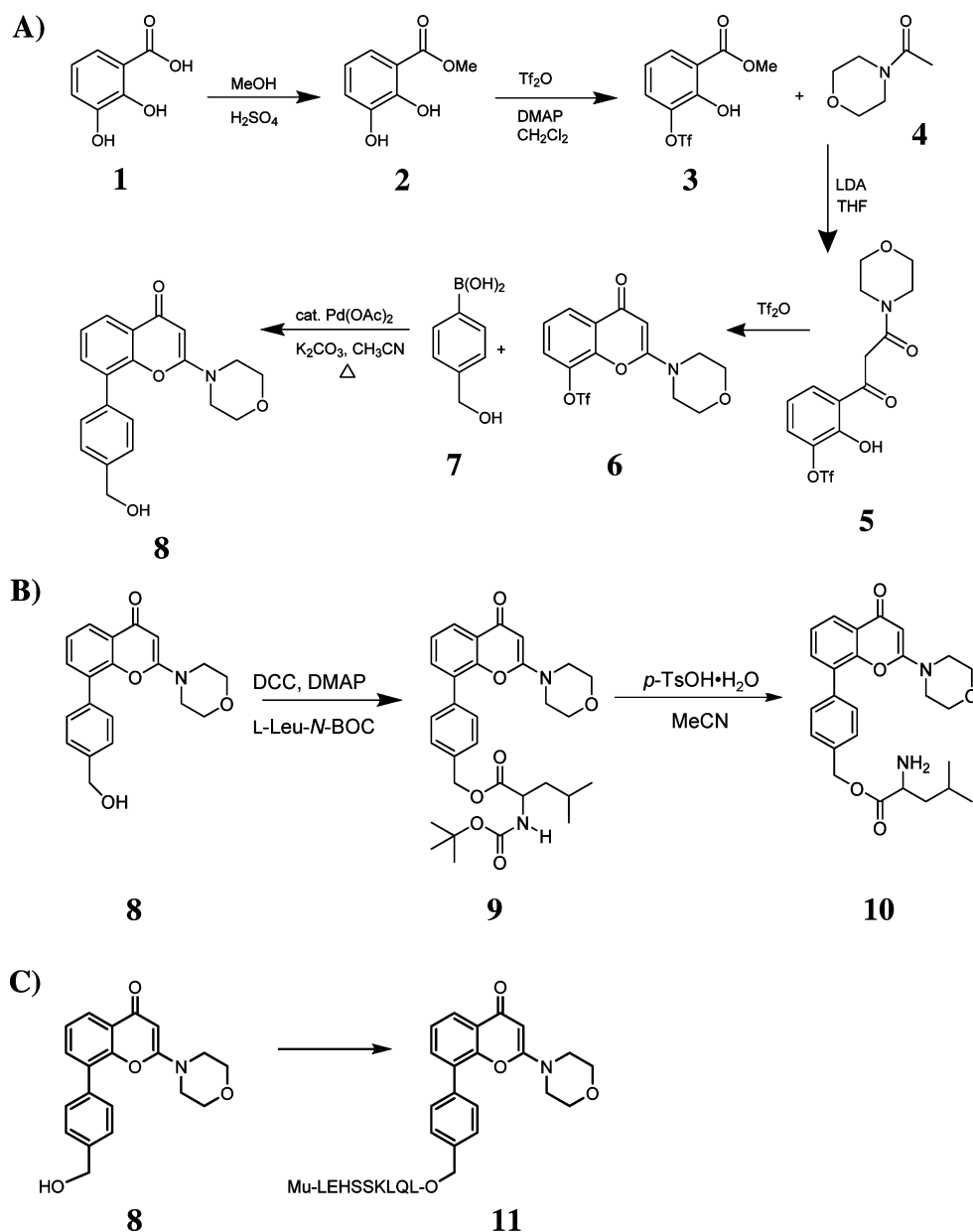


Figure 2. Synthesis of LY294002 analogues. Once **8** was prepared (panel A), it was used to attach leucine, generating **10** (panel B), or the Mu-LEHSSKLQ-peptide (panel C), generating **11**, the PI3K inhibitor prodrug.

subjected to Suzuki coupling with commercially available 4-(hydroxymethyl)phenylboronic acid (**7**) to produce **8**. Once the LY294002 analogue with the primary alcohol functional group (**8**) was prepared, it could be used to attach the leucine or the Mu-LEHSSKLQ-peptide (Figure 2B,C).

First, we synthesized 4-(2-morpholino-4-oxo-4H-chromen-8-yl)benzyl-2-(*tert*-butoxycarbonylamino)-4-methylpentanoate (**9**), where **8** is directly attached to BOC-protected leucine. The BOC protecting group can be removed by *p*-TsOH when desired to produce 4-(2-morpholino-4-oxo-4H-chromen-8-yl)benzyl-2-amino-4-methylpentanoate (**10**). **10** represents what would remain after PSA has cleaved off the substrate peptide from the prodrug. The peptide Mu-LEHSSKLQ was attached to **8** by AnaSpec, Inc. (Fremont, CA), to yield Mu-LEHSSKLQ-8-(4-(hydroxymethyl)phenyl)-2-morpholino-4H-chromen-4-one (**11**) as a white powder. Mass calculated as

1487.7 was found to be 1488.0 by LC-MS analysis, conducted at AnaSpec, Inc. (provided with the certificate of analysis).

■ BIOLOGICAL RESULTS

Compound 10 Inhibits the PI3 Kinase. The androgen-independent prostate cancer C4-2 cells that secrete PSA were chosen for this study as a model of advanced and PSA-secreting prostate cancer and used for a preliminary experiment. In parallel, as a negative control, we used the breast cancer BT-549 cell line, which does not secrete PSA. Both cell lines are PTEN-deficient and show constitutive activation of the PI3K/Akt signaling pathway.

As reported, PSA is predicted to cleave **11** after the glutamine, leaving a leucine attached to the phenyl ring of the LY294002. We started by testing whether the “activated prodrug” **10** retained inhibitory properties toward PI3K

inhibition, similarly to unmodified LY294002, as predicted by AutoDock modeling.

The activated prodrug **10** inhibited the PI3 kinase with a potency comparable to that of LY294002, resulting in a dose-dependent reduction of p-Akt T308 levels in both cell lines 30 min after administration (Figure 3). Dose–response analysis shows that 30 μM **10** completely inhibited Akt phosphorylation in both cell lines.

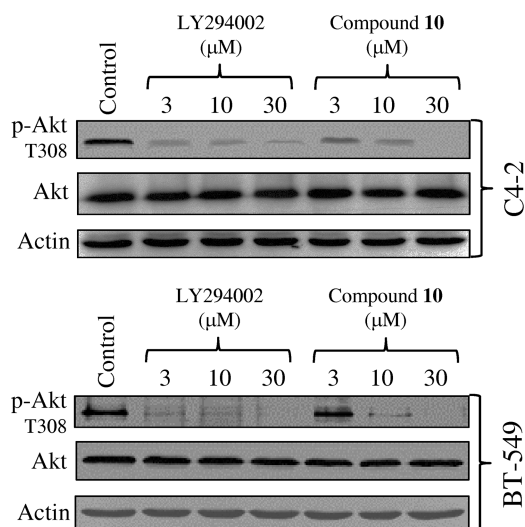


Figure 3. Compound **10** exerts PI3K inhibitory properties similar to those of LY294002. At 30 min after the administration of the LY294002 or compound **10**, the “activated prodrug”, dose-dependent decreases of p-Akt T308 were detected both in prostate cancer C4-2 and in breast cancer BT-549 cells versus control (cells treated with DMSO). Similar results were obtained in three independent experiments.

Compound 11 Inhibits the PI3 Kinase in PSA-Secreting Prostate Cancer Cells. Effects of **11** were monitored in prostate cancer C4-2 and breast cancer BT-549 cells from 30 min to 6 h. A time-dependent reduction of p-Akt T308 levels was observed in prostate cancer C4-2 cells versus control (cells treated with DMSO). Notably, no significant differences in p-Akt T308 levels were detected in breast cancer BT-549 cells treated with **11** during this time period (Figure 4A). To determine whether PI3 kinase inhibition is due to the cleavage of Mu-LEHSSKLQL peptide by PSA and conversion of **11** into **10**, we monitored concentrations of **10** in the media conditioned by either prostate cancer C4-2 or breast cancer BT-549 cells. LC-ESI-MS analysis showed a significant increase of **10** in the media conditioned by prostate cancer C4-2 cells (that secrete PSA) at 30 min and 3 and 6 h after administration, whereas no significant increase was found in the media conditioned by breast cancer BT-549 cells compared to control (cells treated with PBS) (Figure 4B). In addition, the tPSA assay confirmed that during these time points, PSA concentrations were significantly increased in prostate cancer C4-2 conditioned media, whereas no PSA was detected in breast cancer BT-549 conditioned media (Figure 4C). These results suggest that PSA–peptide cleavage is required for activation of **11**.

To further demonstrate that inhibition of the PI3K/Akt pathway by **11** depends on the presence of PSA in the media, we incubated **11** in the medium conditioned by prostate cancer C4-2 cells and then, after an incubation of 6 h, we transferred

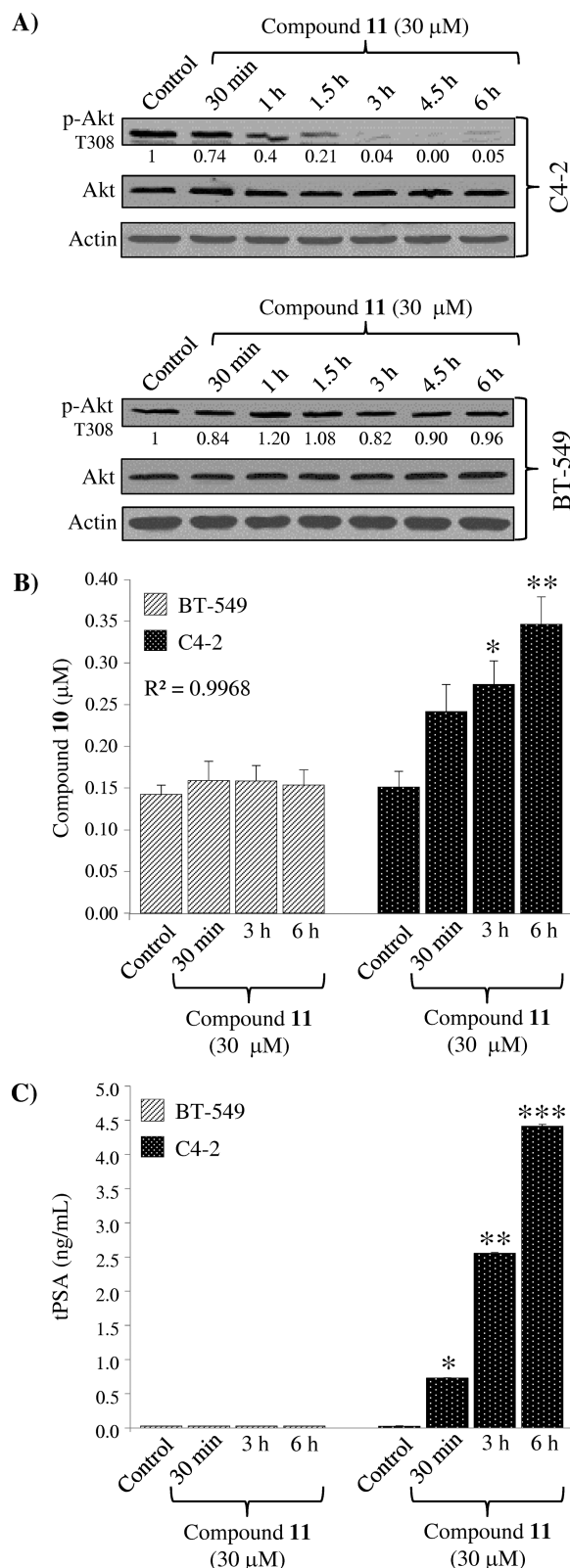


Figure 4. Compound **11** selectively inhibits PI3 kinase in PSA-secreting prostate cancer cells. (A) Prostate cancer C4-2 and breast cancer BT-549 cells were treated with **11** for indicated periods of time. Time-dependent reduction of p-Akt T308 was seen in prostate cancer C4-2 cells (top panel). No significant differences in p-Akt T308 levels were detected in breast cancer BT-549 cells treated with **11** in the same time frame (bottom panel). A representative Western blot, of three independent experiments, is shown. (Control = cells treated with

Figure 4. continued

PBS.) (B) LC-ESI-MS analysis of cell media treated with **11** showed significantly increased concentrations of **10** in the media conditioned by C4-2 cells, but no increase in BT-549 conditioned media. Results are expressed as the mean \pm SEM, $n = 3$; (*) $p < 0.039$ and (**) $p < 0.012$ versus control, represented by BT-549 or C4-2 conditioned media. (C) Total PSA assay (tPSA) showing significant increase of secreted PSA in prostate cancer C4-2 cells in conditioned media. No PSA was detected in breast cancer BT-549 cells conditioned media. Results are expressed as the mean \pm SEM, $n = 3$; (*) $p < 1.1 \times 10^{-5}$, (**) $p < 4.1 \times 10^{-6}$, and (***) $p < 3.26 \times 10^{-5}$ versus control, represented by BT-549 or C4-2 media treated with $30 \mu\text{M}$ **11**.

the C4-2 conditioned media (containing also **11** activated by PSA cleavage) into Petri dishes containing breast cancer BT-549 cells. As shown in Figure 5A, addition of **11** previously

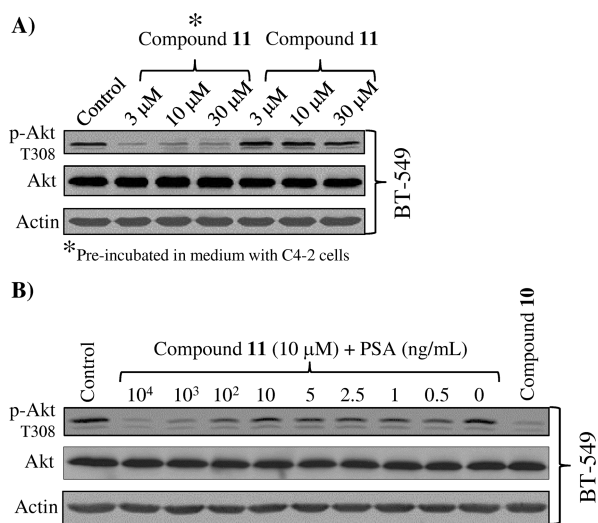


Figure 5. PSA converts compound **11** into an active PI3K inhibitor. (A) Addition of **11** (incubated for 6 h in media conditioned by prostate cancer C4-2 cells) resulted in significant reduction of p-Akt T308 in breast cancer BT-549 cells. (Control = cells treated with PBS.) (B) Compound **11** incubated for 6 h with a range of concentrations (0 – 10^4 ng/mL) of active PSA and added to breast cancer BT-549 cell media for 30 min resulted in significant decreases of p-Akt T308, if compared to control. (Control = cells treated with DMSO.) Similar results were obtained in three independent experiments.

incubated in the media conditioned by prostate cancer C4-2 cells significantly reduced p-Akt T308 levels in breast cancer BT-549 cells (which do not secrete PSA). In contrast, **11** incubated in the media conditioned by breast cancer BT-549 cells had no effects on p-Akt T308 levels. Finally, to confirm that inhibition of PI3K activity by **11** was due to peptide cleavage by PSA (and not by unrelated proteases secreted by prostate cancer C4-2 cells), **11** was incubated for 6 h at 37°C with increasing concentrations of enzymatically active PSA purified from human semen. Addition of **11** (preincubated with PSA) to BT-549 cells for 30 min reduced p-Akt T308 levels in a PSA dose-dependent fashion (Figure 5B). Notably, **11** without enzymatically active PSA had no effect on p-Akt T308 levels in BT-549 cells.

To further demonstrate that activation of **11** is PSA-dependent, we extended the screening to hormone-sensitive prostate cancer LNCaP cells (that secrete PSA) and to

glioblastoma-astrocytoma U-87 MG cells that do not secrete PSA (Figure 6A,B). Consistent with earlier results, p-Akt T308 levels were reduced in LNCaP cells incubated with **11** and in C4-2 cells in a dose-dependent fashion (Figure 6A). This effect was not seen in U-87 MG cells or in BT-549 cells (Figure 6B), supporting the notion that secretion of PSA in the media (confirmed by tPSA assay) (Figure 6C) is needed to cleave the Mu-LEHSSKLQL peptide.

Compound 11 Promotes Apoptosis in C4-2LucBAD Prostate Cancer Cells. As we have previously shown, LY294002 induces apoptosis in C42LucBAD cells that ectopically express BAD, a BH3-only pro-apoptotic protein of the Bcl-2 family.^{18–21}

Administration of **11** inhibited the PI3K/Akt pathway and induced apoptosis in C42LucBAD cells, as evident from increased caspase 3 activity and cleavage of caspase substrate PARP (Figure 7). Somewhat lower levels of caspase activity induced by **11** are likely due to extra time needed for conversion of **11** into an active PI3K inhibitor. These experiments unequivocally demonstrate that **11** is converted by PSA cleavage into an active PI3K inhibitor that selectively blocks the PI3K/Akt pathway and induces apoptosis in PSA-secreting prostate cancer cells.

DISCUSSION AND CONCLUSIONS

In this paper, we have demonstrated for the first time the conversion of a non-tissue-specific PI3K inhibitor (LY294002) into an inactive and latent prodrug (**11**), which can be specifically activated by the PSA protease. Earlier publications have shown that various nonspecific cytotoxic drugs, including thapsigargin, 5-fluorodeoxyuridine, and doxorubicin, could be converted into inactive prodrugs by attaching a PSA-cleavable substrate peptide; however, no publications have reported an attempt to convert a PI3 kinase inhibitor (or any kinase inhibitor) into latent prodrugs activated by PSA cleavage.^{22–24} Converting a PI3K inhibitor into a latent and prostate cancer-specific prodrug may allow an increased drug dosage, accomplishing complete inhibition of PI3K activity in prostate cancer cells while at the same time reducing systemic cytotoxic effects exerted by non-tissue-specific PI3K inhibitors. Compared to nontargeted PI3K inhibitors, a PI3K inhibitor prodrug is expected to be more effective against prostate tumors with a constitutively activated PI3K pathway, which become dependent on PI3K signaling for their growth and survival.^{25,26}

Although this narrows the spectrum of potentially targeted tumors compared to “nonspecific” cytotoxic drugs, there are several advantages of targeting the PI3K signaling pathway in prostate cancer. First, normal tissues do not require constitutive PI3K activity; thus, the presence of the PI3K inhibitor outside tumor sites is not expected to produce substantial toxic side effects, as evident from phase I clinical trials with several nontargeted PI3K inhibitors.^{27,28} Second, as constitutively activated PI3K activity is connected with increased resistance to apoptosis in prostate cancer, a prostate cancer-selective PI3K inhibitor is expected to sensitize prostate tumors to other anticancer therapeutics.^{29,30} Third, as the PI3K inhibitor prodrug cannot enter into cells (and be metabolized) until “released” from inhibiting peptide, these agents should have an improved pharmacokinetic profile compared to unmodified PI3K inhibitor, as reported for SF1126, a LY294002 derivative coupled with a RGDS peptide.¹⁴ Also, unlike the original LY294002, which has poor water solubility and must be dissolved in dimethyl sulfoxide, the peptide-coupled prodrug-

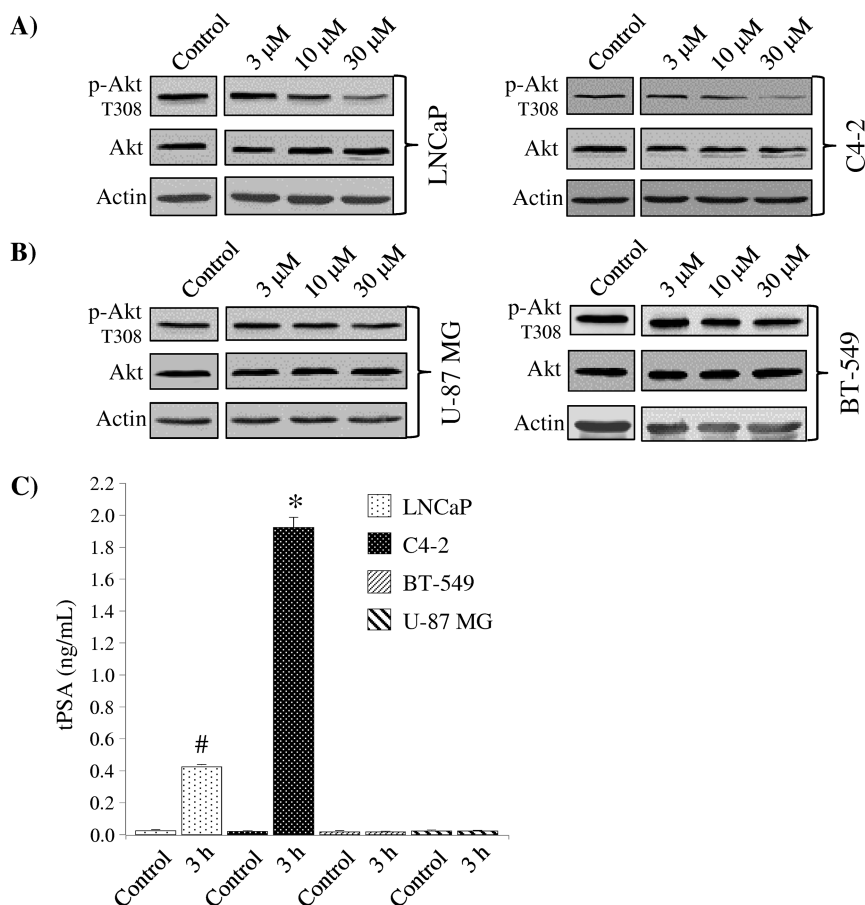


Figure 6. Selective inhibition of PI3K in PSA-secreting prostate cancer cells by compound **11**. (A) Incubation of prostate cancer LNCaP cells and C4-2 cells with **11** at 3 h resulted in a dose-dependent reduction of p-Akt T308 levels. (Control = cells treated with PBS.) (B) No significant reduction of p-Akt T308 levels was observed in glioblastoma-astrocytoma U-87 MG cells or breast cancer BT-549 cells. (Control = cells treated with PBS.) Similar results were obtained in three independent experiments. (C) Total PSA (tPSA) assay confirms secretion of PSA in prostate cancer LNCaP and C4-2 cell media at 3 h. (Control = cell media.) As expected, breast cancer BT-549 and glioblastoma-astrocytoma U-87 MG cells did not secrete PSA. Results are expressed as the mean \pm SEM, $n = 3$; (#) $p < 4.2 \times 10^{-9}$ and (*) $p < 6.3 \times 10^{-10}$ versus control.

LY294002 here presented is water-soluble and, thus, could be more easily formulated as an orally or intravenously delivered therapeutic.

Future experiments in mouse models of prostate cancer will examine pharmacokinetics, pharmacodynamics, and antitumor effects of **11**. Should these experiments demonstrate superior properties of **11** compared to unmodified LY294002, it will justify modification of other PI3K inhibitors into PSA-activated prodrugs and clinical testing of these new prodrug-PI3K inhibitors in patients with advanced prostate cancer. Activating mutations of PI3K pathway are observed in almost all advanced prostate tumors; therefore, introducing improved prostate-selective PI3K inhibitors into the clinic may benefit a substantial number of prostate cancer patients.

EXPERIMENTAL SECTION

Chemical Synthesis. 8-(4-(Hydroxymethyl)phenyl)-2-morpholino-4H-chromen-4-one (**8**). 2-Morpholin-4-yl-4-oxo-4H-chromen-8-yl trifluoromethanesulfonate, **7** (100 mg, 0.263 mmol), was dissolved in 5:1 MeCN/EtOH (10 mL). K_2CO_3 (2.5 equiv, 0.091 g, 0.658 mmol) was added, and the solution was degassed with N_2 . 4-(Hydroxymethyl)phenylboronic acid (1.21 equiv, 0.048 g, 0.318 mmol) and $Pd(OAc)_2$ (0.1 equiv, 0.006 g, 0.0263 mmol) were added, and the solution was refluxed overnight. The solution was cooled to room temperature, filtered through Celite, washed with MeCN (10 mL), and dried with Na_2SO_4 . The reaction mixture was

condensed by rotary evaporation and purified on alumina using 95:5 ethyl acetate/ethanol as an eluent to give 8-(4-(hydroxymethyl)phenyl)-2-morpholino-4H-chromen-4-one as a pale yellow powder (0.062 g, 0.184 mmol, 67%): R_f 0.5 (95:5 ethyl acetate/ethanol); 1H NMR (300 MHz, $CDCl_3$) δ 8.18 (dd, $J = 1.7, 7.9$ Hz, 1H), 7.50 (m, 6H), 5.52 (s, 1H), 4.80 (s, 2H), 3.74 (t, $J = 4.8$ Hz, 4H), 3.36 (t, $J = 5.1$ Hz, 4H); ^{13}C NMR (75.47 MHz, $CDCl_3$) δ 177.23, 162.57, 150.57, 140.93, 135.49, 133.56, 130.03, 129.46, 126.82, 125.05, 124.76, 123.35, 87.03, 65.88, 64.75, 44.74. HRMS $[M + H]^+$ calculated for $C_{20}H_{19}NO_4$, 338.1392; found, 338.1393.

4-(2-Morpholino-4-oxo-4H-chromen-8-yl)benzyl-2-(tert-butoxycarbonylamino)-4-methylpentanoate (**9**). 8-(4-(Hydroxymethyl)phenyl)-2-morpholino-4H-chromen-4-one, **8** (0.259 g, 0.766 mmol), was dissolved in DCM (20 mL). *N*- α -tert-Butoxycarbonyl-L-leucine (2 equiv, 0.354 g, 1.532 mmol), DCC (2 equiv, 0.316 g, 1.532 mmol), and DMAP (1 equiv, 0.094 g, 0.766 mmol) were added, and the solution was stirred at room temperature overnight. DCM (90 mL) was added, and the solution was washed with cold 1 M HCl (80 mL), $NaHCO_3$ (60 mL), and brine (60 mL). Organic fractions were dried with Na_2SO_4 , and the reaction mixture was condensed by rotary evaporation and purified on alumina using ethyl acetate as an eluent to give 4-(2-morpholino-4-oxo-4H-chromen-8-yl)benzyl-2-(tert-butoxycarbonylamino)-4-methylpentanoate as a clear oil (0.161 g, 0.293 mmol, 38%): R_f 0.6 (100% ethyl acetate); 1H NMR (300 MHz, $CDCl_3$) δ 8.16 (dd, $J = 1.8, 7.8$ Hz, 1H), 7.56–7.37 (m, 6H), 5.52 (s, 1H), 5.22 (s, 2H), 4.96 (d, $J = 8.6$ Hz, 1H), 4.37 (m, 1H), 3.73 (t, $J = 4.4$ Hz, 4H), 3.34 (t, $J = 4.9$ Hz, 4H), 2.03 (m, 2H), 1.62 (m, 1H), 1.43 (s, 9H), 0.92 (dd, $J = 1.1, 6.5$ Hz, 6H); ^{13}C NMR (75.47 MHz,

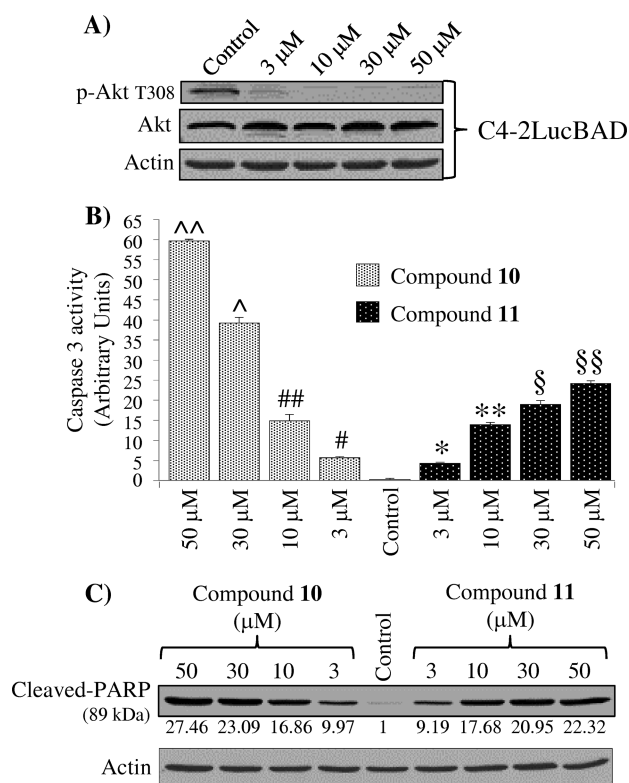


Figure 7. Compound 11 induces apoptosis in C4-2LucBAD cells. (A) Compound 11 induced a dose-dependent reduction of p-Akt T308 in C4-2LucBAD cells in 3 h. (Control = cells treated with PBS.) (B) Caspase 3 assay performed in C4-2LucBAD cells 6 h after the administration of 10 and 11. Results are expressed as the mean \pm SEM, $n = 2$; (#) $p < 0.0062$, (##) $p < 0.012$; (\wedge) $p < 0.0015$; ($\wedge\wedge$) $p < 8.3 \times 10^{-5}$, (*) $p < 0.0055$, (**) $p < 0.0022$, (§) $p < 0.003$, and (§§) $p < 0.001$ versus control. (Control = cells treated with DMSO.) (C) Samples from (B) were analyzed for the cleaved PARP (89 kDa), confirming activation of caspases effector after the administration of 10 or 11. (Control = cells treated with DMSO.) Similar results were obtained in three independent experiments.

CDCl_3) δ 177.10, 173.37, 162.48, 155.39, 150.47, 136.25, 135.38, 133.47, 129.50, 127.94, 125.18, 124.75, 123.31, 87.02, 79.90, 66.34, 65.84, 52.13, 44.66, 41.58, 28.25, 24.75, 22.81, 21.82. HRMS [$M + \text{Na}$] $^+$ calculated for $\text{C}_{31}\text{H}_{38}\text{N}_2\text{O}_7$, 573.2577; found, 573.2643.

4-(2-Morpholino-4-oxo-4H-chromen-8-yl) benzyl-2-amino-4-methylpentanoate (10). 4-(2-Morpholino-4-oxo-4H-chromen-8-yl) benzyl-2-(*tert*-butoxycarbonylamino)-4-methylpentanoate, 9 (0.070 g, 0.127 mmol), was dissolved in MeCN (15 mL). *p*-TsOH \cdot H $_2$ O (2 equiv, 0.044 g, 0.254 mmol) was added and the solution stirred at room temperature for 42 h. *p*-TsOH \cdot H $_2$ O (1 equiv, 0.022 g, 0.127 mmol) was added and the solution stirred for an additional 23 h. The reaction mixture was condensed by rotary evaporation. The solid residue was dissolved in cold H $_2$ O (6 mL), and ethyl acetate (10 mL) was added. The aqueous layer was separated, and saturated NaHCO $_3$ (5 mL) was added. An aqueous layer was extracted with ethyl acetate (3 \times 10 mL). Organic fractions were dried with Na $_2$ SO $_4$, and solvent was removed by rotary evaporation to give 4-(2-morpholino-4-oxo-4H-chromen-8-yl)benzyl 2-amino-4-methylpentanoate as a white solid (0.033 g, 0.073 mmol, 58%): ^1H NMR (300 MHz, CDCl_3) δ 8.16 (dd, $J = 1.6, 7.8$ Hz, 1H), 7.46 (m, 6H), 5.52 (s, 1H), 5.22 (s, 2H), 3.71 (t, $J = 4.8$ Hz, 4H), 3.57 (m, 1H), 3.34 (t, $J = 5.0$ Hz, 4H), 1.91 (m, 2H), 1.62 (m, 1H), 0.91 (t, $J = 6.5$ Hz, 6H); ^{13}C NMR (75.47 MHz, CDCl_3) δ 177.53, 176.60, 162.93, 150.93, 136.78, 136.04, 133.91, 130.12, 130.00, 128.52, 125.66, 125.21, 123.77, 87.50, 66.55, 66.29, 45.13, 44.48, 29.17, 25.19. HRMS [$M + \text{H}$] $^+$ calculated for $\text{C}_{26}\text{H}_{30}\text{N}_2\text{O}_5$, 451.2233; found, 451.2302.

The purity of compounds was measured by LC-ESI-MS analysis using an Accela Open 1200 UHPLC coupled to an LTQ XL Orbitrap mass spectrometer (Thermo Fisher Scientific, Waltham, MA, USA), resulting to be $\geq 95\%$. The purity of 11 was $>95\%$ after LC-ESI-MS analysis, conducted at AnaSpec, Inc., as verified by the certificate of analysis.

Cell Cultures. The hormone-responsive prostate cancer LNCaP and breast cancer BT-549 cell lines were purchased from ATCC (Manassas, VA, USA). The androgen-independent prostate cancer LNCaP subline C4-2 and the glioblastoma-astrocytoma U-87 MG cells were generous gifts from Dr. Leland Chung (Cedars-Sinai Medical Center, Los Angeles, CA, USA) and Dr. Frank Furnari (University of California, San Diego, CA, USA), respectively.

All cells were maintained in a humidified atmosphere (5% CO $_2$) at 37 $^\circ\text{C}$, using RPMI 1640 (C4-2, C4-2LucBAD, and BT-549), T-Medium (LNCaP), and DMEM (U-87 MG) supplemented with 10% FBS (5% for LNCaP). BT-549 medium was also supplemented with 0.023 U/mL of insulin. All tissue culture reagents were purchased from Invitrogen (Carlsbad, CA, USA).

Experimental Setup. If not otherwise indicated, cells were seeded at $4 \times 10^5/6$ cm Petri dish and kept in culture for 48 h to reach about 80% confluence before the start of any experiments. Cells were kept in a serum-free media condition (LNCaP cells were kept in medium supplemented with 2.5% FBS). C4-2LucBAD cells were kept in serum-free medium for 18 h to increase PSA concentration.

Total PSA Electrochemiluminescence Immunoassay. Total PSA was assayed with a Cobas Elecsys Total PSA according to the manufacturer's protocol, using a Roche Elecsys 2010 Chemistry Analyzer (Roche, Basel, Switzerland). Each sample was assayed in triplicate.

Western Blotting. Media were removed and cells washed gently two times using cold phosphate-buffered saline (PBS) on ice. Lysates were generated using cold 20 mM HEPES, 150 mM NaCl, 1 mM EDTA, 0.5% Na $^+$ deoxycholate, 1% Nonidet P-40, and 1 mM DTT, pH 7.4, buffer containing protease inhibitors (10 $\mu\text{g}/\text{mL}$ aprotinin, 10 $\mu\text{g}/\text{mL}$ leupeptin, 10 $\mu\text{g}/\text{mL}$ pepstatin, 1 mM benzamide, and 1 mM PMSF) and phosphatase inhibitors (1 mM NaVO $_4$, 50 mM β -glycerophosphate, 40 mM *p*-nitrophenylphosphate, 40 mM NaF, and 1 $\mu\text{g}/\text{mL}$ microcystin). All reagents were purchased from Sigma-Aldrich (St. Louis, MO, USA). Cell lysates were clarified by centrifugation at 15000 rpm for 15 min at 4 $^\circ\text{C}$, and the supernatant was collected and protein content measured by a Bradford assay (Bio-Rad Laboratories, Hercules, CA, USA) according to the manufacturer's directions. Proteins were separated on SDS-PAGE on 12% gels and transferred onto a 0.45 μm nitrocellulose membrane (PerkinElmer, Waltham, MA, USA). Western blotting was performed with the Odyssey CLx Infrared Imaging System (Li-Cor Biosciences, Lincoln, NE, USA), according to the manufacturer's instructions. Rabbit polyclonal anti-p-Akt Thr308, anti-Akt, and anti-cleaved PARP (Asp214) were purchased from Cell Signaling Technology (Beverly, MA, USA). Mouse monoclonal anti- β -actin was purchased from Sigma-Aldrich. Secondary goat anti-mouse IRDye 680 and goat-anti-rabbit IRDye 800 were both purchased from Li-Cor Biosciences. Protein bands were quantified using ImageJ software (National Institutes of Health, Bethesda, MD, USA).

Caspase 3 Assay. Apoptosis in whole cell populations was assessed by monitoring caspase 3 activity with the specific fluorogenic substrate Ac-DEVD-7-amido-4-trifluoromethylcoumarin (Bachem, Torrance, CA, USA), as previously reported.³⁰ On ice, adherent and floating cells were collected and lysed using a cold lysis buffer (1% Nonidet P-40, 150 mM NaCl, 20 mM HEPES, 1 mM EDTA, 1 mM DTT, and 5 $\mu\text{g}/\text{mL}$ aprotinin, leupeptin, and pepstatin, respectively). Fluorescence was recorded each 15 min for 1 h using a VersaFluor (Bio-Rad). Caspase 3 activity was expressed in arbitrary units and calculated using Excel 2010 (Microsoft Corp., Redmond, WA, USA).

LC-ESI-MS Analysis. LC-ESI-MS analysis was performed using an Accela Open 1200 UHPLC coupled to an LTQ XL Orbitrap mass spectrometer (Thermo Fisher Scientific). Separation was accomplished using a Zorbax Eclipse XDB-C18 (1.8 μm , 2.1 \times 50 mm) analytical column with a Zorbax extend C18 narrow-bore guard

column (5 μm , 2.1 \times 12.5 mm) (Agilent Technologies, Santa Clara, CA, USA). The following mobile phases were used for the separation: solvent A, water/0.1% formic acid; and solvent B, methanol/0.1% formic acid. The gradient used for separation was 95 to 5% solvent A over 10 min at a flow rate of 250 $\mu\text{L}/\text{min}$. Using the mass of 496.2569 \pm 0.005, optimized positive mode ESI conditions were found as follows: sheath and auxiliary gas, 60 and 4 arbitrary units, respectively; spray voltage, 4 kV; capillary temperature and voltage, 325 $^{\circ}\text{C}$ and 49 V, respectively; tube lens voltage, 115 V. Full scan high-resolution mass spectra were collected at 60000 Hz from m/z 150 to 2000. The full scan data for standard curve samples and unknowns were processed with Xcalibur software to determine concentrations (Thermo Fisher Scientific).

C4-2 Conditioned Medium Assay. C4-2 and BT-549 cells were cultured as described above. **11** was added to the medium with C4-2 cells and incubated for 6 h at 37 $^{\circ}\text{C}$ in a humidified atmosphere (5% CO_2) in serum-free medium. Medium was then collected and added to BT-549 cells for 3 h. Inhibition of the PI3 kinase pathway was followed by monitoring the p-Akt T308 levels by Western blotting.

Cleavage of Compound 11 with Purified PSA. Compound **11** was incubated in 50 mM Tris-HCl–0.1 M NaCl, pH 7.8, buffer for 6 h at 37 $^{\circ}\text{C}$ with purified active human PSA (Merck, Darmstadt, Germany) and then added to BT-549 cells for 30 min, cultured as previously described. Inhibition of PI3 kinase was followed by monitoring p-Akt T308 levels by Western blotting.

Statistical Analysis. Probability (p) values were calculated using the ANOVA one-way test; p values ≤ 0.05 were considered to be statistically significant. The results are expressed as the mean \pm SEM, $n = 3$.

AUTHOR INFORMATION

Corresponding Author

*(M.E.W.) Phone: +1-(336)-758-3898. E-mail: welker@wfu.edu (G.K.) Phone: +1-(336)-713-7650. E-mail: gkulik@wakehealth.edu.

Notes

The authors declare no competing financial interest.

ACKNOWLEDGMENTS

We thank Dr. Marcus W. Wright (Wake Forest University, Department of Chemistry) for LC-ESI-MS analysis, Tina Snider (Department of Urology, Wake Forest Baptist Health) for performing ECLIA tPSA assays, and Karen Kline for editing. This work was supported by WFU Cross-Campus Collaborative Research Program and R01CA118329 to G.K.

ABBREVIATIONS USED

BAD, Bcl-2-associated death promoter; Bcl-2, B-cell lymphoma 2; Bcl-X_L, B-cell lymphoma extra-large; DCC, *N,N'*-dicyclohexylcarbodiimide; DCM, dichloromethane; DMAP, 4-dimethylaminopyridine; DMSO, dimethyl sulfoxide; DTT, dithiothritol; PARP, poly(ADP-ribose) polymerase; PBS, phosphate buffer saline; PI3K, phosphatidylinositol-3-kinase; PSA, prostate-specific antigen; PTEN, phosphatase and tensin homologue deleted on chromosome 10

REFERENCES

- (1) Wang, X.; Ma, D.; Olson, W. C.; Heston, W. D. In vitro and in vivo responses of advanced prostate tumors to PSMA ADC, an auristatin-conjugated antibody to prostate-specific membrane antigen. *Mol. Cancer Ther.* **2011**, *10*, 1728–1739.
- (2) Sarker, D.; Reid, A. H. M.; Yap, T. A.; de Bono, J. S. Targeting the PI3K/AKT pathway for the treatment of prostate cancer. *Clin. Cancer Res.* **2009**, *15*, 4799–4805.

- (3) Cohen, M. B.; Rokhlin, O. W. Mechanisms of prostate cancer cell survival after inhibition of AR expression. *J. Cell Biochem.* **2009**, *106*, 363–371.

- (4) Morgan, T. M.; Koreckij, T. D.; Corey, E. Targeted therapy for advanced prostate cancer: inhibition of the PI3K/Akt/mTOR pathway. *Curr. Cancer Drug Targets* **2009**, *9*, 237–249.

- (5) Mazzeletti, M.; Bortolin, F.; Brunelli, L.; Pastorelli, R.; Di Giandomenico, S.; Erba, E.; Ubezio, P.; Broggin, M. Combination of PI3K/mTOR inhibitors: antitumor activity and molecular correlates. *Cancer Res.* **2011**, *71*, 4573–4584.

- (6) Erlich, R. B.; Kherrouche, Z.; Rickwood, D.; Endo-Munoz, L.; Cameron, S.; Dahler, A.; Hazar-Rethinam, M.; de Long, L. M.; Wooley, K.; Guminski, A.; Saunders, N. A. Preclinical evaluation of dual PI3K-mTOR inhibitors and histone deacetylase inhibitors in head and neck squamous cell carcinoma. *Br. J. Cancer* **2012**, *106*, 107–115.

- (7) Bjork, T.; Lilja, H.; Christensson, A. The prognostic value of different forms of prostate specific antigen and their ratios in patients with prostate cancer. *BJU Int.* **1999**, *84*, 1021–1027.

- (8) LeBeau, A. M.; Singh, P.; Isaacs, J. T.; Denmeade, S. R. Prostate-specific antigen is a “chymotrypsin-like” serine protease with unique P1 substrate specificity. *Biochemistry* **2009**, *48*, 3490–3496.

- (9) Evans-Axelsson, S.; Ulmert, D.; Orbom, A.; Peterson, P.; Nilsson, O.; Wennerberg, J.; Strand, J.; Wingardh, K.; Olsson, T.; Hagman, Z.; Tolmachev, V.; Bjartell, A.; Lilja, H.; Strand, S. E. Targeting free prostate-specific antigen for in vivo imaging of prostate cancer using a monoclonal antibody specific for unique epitopes accessible on free prostate-specific antigen alone. *Cancer Biother. Radiopharm.* **2012**, *27*, 243–251.

- (10) Coombs, G. S.; Bergstrom, R. C.; Pellequer, J. L.; Baker, S. I.; Navre, M.; Smith, M. M.; Tainer, J. A.; Madison, E. L.; Corey, D. R. Substrate specificity of prostate-specific antigen (PSA). *Chem. Biol.* **1998**, *5*, 475–488.

- (11) LeBeau, A. M.; Banerjee, S. R.; Pomper, M. G.; Mease, R. C.; Denmeade, S. R. Optimization of peptide-based inhibitors of prostate-specific antigen (PSA) as targeted imaging agents for prostate cancer. *Bioorg. Med. Chem.* **2009**, *17*, 4888–4893.

- (12) Vlahos, C. J.; Matter, W. F.; Brown, R. F.; Traynor-Kaplan, A. E.; Heyworth, P. G.; Prossnitz, E. R.; Ye, R. D.; Marder, P.; Schelm, J. A.; Rothfuss, K. J.; Serlin, B. S.; Simpson, P. J. Investigation of neutrophil signal transduction using a specific inhibitor of phosphatidylinositol 3-kinase. *J. Immunol.* **1995**, *154*, 2413–2422.

- (13) Holmes, D. PI3K pathway inhibitors approach junction. *Nat. Rev. Drug Discov.* **2011**, *10*, 563–564.

- (14) Garlich, J. R.; De, P.; Dey, N.; Su, J. D.; Peng, X.; Miller, A.; Murali, R.; Lu, Y.; Mills, G. B.; Kundra, V.; Shu, H. K.; Peng, Q.; Durden, D. L. A vascular targeted pan phosphoinositide 3-kinase inhibitor prodrug, SF1126, with antitumor and antiangiogenic activity. *Cancer Res.* **2008**, *68*, 206–215.

- (15) Gharbi, S. I.; Zvelebil, M. J.; Shuttleworth, S. J.; Hancox, T.; Saghiri, N.; Timms, J. F.; Waterfield, M. D. Exploring the specificity of the PI3K family inhibitor LY294002. *Biochem. J.* **2007**, *404*, 15–21.

- (16) Morris, G. M.; Goodsell, D. S.; Halliday, R. S.; Huey, R.; Hart, W. E.; Belew, R. K.; Olson, A. J. Automated docking using a Lamarckian genetic algorithm and an empirical binding free energy function. *J. Comput. Chem.* **1998**, 1639–1662.

- (17) Abbott, B. M.; Thompson, P. E. Synthetic studies of the phosphatidylinositol 3-kinase inhibitor LY294002 and related analogues. *Aust. J. Chem.* **2003**, *56*, 1099–1106.

- (18) Zha, J.; Harada, H.; Yang, E.; Jockel, J.; Korsmeyer, S. J. Serine phosphorylation of death agonist BAD in response to survival factor results in binding to 14-3-3 not BCL-X(L). *Cell* **1996**, *87*, 619–628.

- (19) Datta, S. R.; Dudek, H.; Tao, X.; Masters, S.; Fu, H.; Gotoh, Y.; Greenberg, M. E. Akt phosphorylation of BAD couples survival signals to the cell-intrinsic death machinery. *Cell* **1997**, *91*, 231–241.

- (20) del Peso, L.; Gonzalez-Garcia, M.; Page, C.; Herrera, R.; Nunez, G. Interleukin-3-induced phosphorylation of BAD through the protein kinase Akt. *Science* **1997**, *278*, 687–689.

- (21) Sastry, K. S. R.; Karpova, Y.; Kulik, G. Epidermal growth factor protects prostate cancer cells from apoptosis by inducing BAD

phosphorylation via redundant signaling pathways. *J. Biol. Chem.* **2006**, *281*, 27367–27377.

(22) Khan, S. R.; Denmeade, S. R. In vivo activity of a PSA-activated doxorubicin prodrug against PSA-producing human prostate cancer xenografts. *Prostate* **2000**, *45*, 80–83.

(23) Brady, S. F.; Pawluczyk, J. M.; Lumma, P. K.; Feng, D. M.; Wai, J. M.; Jones, R.; DeFeo-Jones, D.; Wong, B. K.; Miller-Stein, C.; Lin, J. H.; Oliff, A.; Freidinger, R. M.; Garsky, V. M. Design and synthesis of a pro-drug of vinblastine targeted at treatment of prostate cancer with enhanced efficacy and reduced systemic toxicity. *J. Med. Chem.* **2002**, *45*, 4706–4715.

(24) Denmeade, S. R.; Jakobsen, C. M.; Janssen, S.; Khan, S. R.; Garrett, E. S.; Lilja, H.; Christensen, S. B.; Isaacs, J. T. Prostate-specific antigen-activated thapsigargin prodrug as targeted therapy for prostate cancer. *J. Natl. Cancer Inst.* **2003**, *95*, 990–1000.

(25) Rudner, J.; Ruiner, C. E.; Handrick, R.; Eibl, H. J.; Belka, C.; Jendrossek, V. The Akt-inhibitor Erufosine induces apoptotic cell death in prostate cancer cells and increases the short term effects of ionizing radiation. *Radiat. Oncol.* **2010**, *5*, 108.

(26) Ellwood-Yen, K.; Keilhack, H.; Kunii, K.; Dolinski, B.; Connor, Y.; Hu, K.; Nagashima, K.; O'Hare, E.; Erkul, Y.; Di Bacco, A.; Gargano, D.; Shomer, N. H.; Angagaw, M.; Leccese, E.; Andrade, P.; Hurd, M.; Shin, M. K.; Vogt, T. F.; Northrup, A.; Bobkova, E. V.; Kasibhatla, S.; Bronson, R. T.; Scott, M. L.; Draetta, G.; Richon, V.; Kohl, N.; Blume-Jensen, P.; Andersen, J. N.; Kraus, M. PDK1 attenuation fails to prevent tumor formation in PTEN-deficient transgenic mouse models. *Cancer Res.* **2011**, *71*, 3052–3065.

(27) Yuan, J.; Mehta, P. P.; Yin, M. J.; Sun, S.; Zou, A.; Chen, J.; Rafidi, K.; Feng, Z.; Nickel, J.; Engebretsen, J.; Hallin, J.; Blasina, A.; Zhang, E.; Nguyen, L.; Sun, M.; Vogt, P. K.; McHarg, A.; Cheng, H.; Christensen, J. G.; Kan, J. L.; Bagrodia, S. PF-04691502, a potent and selective oral inhibitor of PI3K and mTOR kinases with antitumor activity. *Mol. Cancer Ther.* **2011**, *10*, 2189–2199.

(28) Brachmann, S. M.; Hofmann, I.; Schnell, C.; Fritsch, C.; Wee, S.; Lane, H.; Wang, S.; Garcia-Echeverria, C.; Maira, S. M. Specific apoptosis induction by the dual PI3K/mTOR inhibitor NVP-BEZ235 in HER2 amplified and PIK3CA mutant breast cancer cells. *Proc. Natl. Acad. Sci. U.S.A.* **2009**, *106*, 22299–22304.

(29) Wallin, J. J.; Edgar, K. A.; Guan, J.; Berry, M.; Prior, W. W.; Lee, L.; Lesnick, J. D.; Lewis, C.; Nonomiya, J.; Pang, J.; Salphati, L.; Olivero, A. G.; Sutherlin, D. P.; O'Brien, C.; Spoerke, J. M.; Patel, S.; Lensun, L.; Kassees, R.; Ross, L.; Lackner, M. R.; Sampath, D.; Belvin, M.; Friedman, L. S. GDC-0980 is a novel class I PI3K/mTOR kinase inhibitor with robust activity in cancer models driven by the PI3K pathway. *Mol. Cancer Ther.* **2011**, *10*, 2426–2436.

(30) Sastry, K. S. R.; Karpova, Y.; Prokopovich, S.; Smith, A. J.; Essau, B.; Gersappe, A.; Carson, J. P.; Weber, M. J.; Register, T. C.; Chen, Y. Q.; Penn, R. B.; Kulik, G. Epinephrine protects cancer cells from apoptosis via activation of cAMP-dependent protein kinase and BAD phosphorylation. *J. Biol. Chem.* **2007**, *282*, 14094–14100.